Int j simul model 21 (2022) 4, 615-626
Original scientific paper

PARAMETRIC OPTIMIZATION OF TWO POINT INCREMENTAL FORMING USING GRA AND TOPSIS

Visagan, A. & Ganesh, P.
Department of Production Technology, MIT Campus, Anna University, Chennai 44, Tamil Nadu, India
E-Mail: visaganarjunan69@gmail.com

Abstract
Different innovative forming methods have been developed in order to make custom made goods at a reasonable cost. Due to stress induced between the tool and die, the procedure facilitates the ability of metal sheets to be formed. The dimensional accuracy of formed items can be improved by selecting the best Two Point Incremental Forming (TPIF) process parameters. In this work, TPIF of SS316L sheets of 0.8 mm was performed by varying the process variables such as die angle, step of forming, rate of feed and tool rotational speed to form a double wall angle circular cone with a forming height of 40 mm. The output responses such as surface roughness and thickness of the formed components were measured. An ANOVA was performed with a confidence level of 95 % to identify the most influential process parameter on the output response. The accuracy of the proposed methods, Grey Relational Analysis (GRA) and TOPSIS, were validated by choosing the optimal process parameter combination resulted from several experimental trial runs.
(Received in July 2022, accepted in September 2022. This paper was with the authors 1 week for 1 revision.)

Key Words: Two Point Incremental Forming, Surface Roughness, Thickness, Taguchi, Grey Relational Analysis, TOPSIS, ANOVA

1. INTRODUCTION

Incremental sheet forming is a novel flexible sheet metal forming technology where sheet metal is formed into the final workpiece by a series of small incremental deformations. The incremental sheet forming process, as one of the research frontiers in the field of rapid sheet metal forming, can form parts with a complex curved surface shape without a special mould or using a simple mould. The conventional sheet forming processes require custom-designed expensive tooling systems for each component to be manufactured. Hence, there is always a need for the development of innovative flexible manufacturing processes for small-quantity production and rapid prototyping of metal and non-metal components. Two Point Incremental Forming (TPIF) process employs a partial or full die to the opposite side of the forming tool to provide support to the sheet specimen. The lower surface of the sheet remains in direct contact with the support. The forming-tool moves from the inside outwards in a planar motion. Step depth is executed by the forming-tool contour by contour in a vertically downward direction synchronously with the perimeter of the sheet. The partial die supports only a specific area of the specimen whereas TPIF with a full die uses different specific support for a particular shape of the component with low cost. The process is termed TPIF due to the fact that two points of the sheet are in contact with forming agents (forming-tool and lower support).

In this work, four different parameters have been considered as input namely Die angle, Step of forming, Rate of feed and Tool rotational speed. The top wall angle of the die is varied having three different angles (70°, 73° and 75°) and the bottom wall angle is kept constant at 66°. The output parameters surface roughness and thickness have been considered for this optimization process.

2. TPIF LEADING EDGE PROCESS

Recently, the incremental forming process emerged as a significant operation for sheet metal applications. Optimization methods are critical for optimizing the process parameters of the Incremental Sheet Forming process [1]. Traditional incremental sheet forming focuses on metal sheet formability considering critical parameters such as sheet thickness, spindle speed, step depth, feed rate, and tool diameter etc. [2]. In order to predict the influence of critical parameters on responses such as the forming forces, thickness distribution and other related outputs, a new software, Tool Motion Points Generator (TMPG), was developed which reduced the simulation time effectively [3]. The response surface approach was developed and studied to optimise the process parameters by taking into consideration the thinning effect [4]. In multi-pass TPIF, the thickness of the walls is made uniform by increasing the number of passes and decreasing the forming angle between passes. The forming tool diameter, feed rate and step size have a significant effect on thickness uniformity in descending order [5].

Forming of AA5083 sheets was performed to study the influence of process parameter responses through ANFIS and response surface methodology. The wall angle and the thickness of the deformed sheet are both affected by the feed rate. The size of the steps has a greater impact on the surface roughness [6]. Simulations were performed on an AA2024 sheet for the TPIF method with a 5.8 % inaccuracy between modelling and experimental data [7]. Experiments were conducted by combining incremental forming with stretch forming to improve the uniform thickness distribution compared to the traditional incremental forming [8]. Lower surface roughness was calculated for optimising aluminium alloy AA2024-O and AA6063-O sheets with flat and hemispherical tool profiles by considering eight input parameters. Results show that the surface roughness is not good enough when a flat-ended tool is used, but it is great when a hemispherical tool is used [9].

Optimization using GRA was implemented for adjusting the process factors on AA1050, DC01, and Cu-Be2. When the interaction property of the process variables was examined, rotational tool speed and feed rate exhibit a strong connection [10]. Using Taguchi analysis experiments were performed on incremental forming on AA2024-O and AA6063-O to determine the forming force. Using a hemispherical tool, the smallest forming force was seen, whereas using a flat-end tool, the greatest forming force was observed [11]. The response surface methodology was implemented to optimise the maximum resultant force and thinning ratio on the TPIF of Aluminium 1050. The thinning ratio was found to be a significant factor for wall angle. Sheet thickness was found to be a significant factor in the forming force [12]. An attempt in using different types of lubrication methods in incremental forming of Aluminium alloy 1060-H22 was experimentally investigated. The lubrication showed a significant impact on thickness distribution and forming force [13]. Additionally, some literature has reported experiments in temperature-controlled environments. Experiments have revealed that the temperature had a notable impact on achieving optimal forming depth and plate thickness at 80 °C [14].

Experimental and theoretical studies have been conducted on the pyramid and cone frustum shapes for various angles. The geometrical accuracy has been improved with the help of the reverse compensation method [15]. Grey relational analysis was used in incremental forming by adjusting the process variables and it was discovered that lubrication was the most influential parameter and feed rate was the least influential component [16]. AA1050-O was subjected to incremental forming utilising DOE to enhance the surface quality and formability. The thickness of the sheet and step depth play a significant role in achieving superior surface quality and enhanced formability. The maximal forming angle decreases as the tool diameter increases [17].

3. EXPERIMENTAL WORK

A 3-axis numerical control vertical machining centre, V-510 Vertimach, with Siemens 828D numerical control system, was used as the forming equipment and is shown in Fig. 1 a. Fig. 1 b shows the Two-Point Incremental Forming experimental set-up mounted on the Computer Numerical Control (CNC) machine. A double wall angle circular cone was selected as the target geometry. The die was modelled using Solid works 2018 for the target geometry. The bottom wall angle was constant at 66° and the top wall angle was varied at 70°, 73° and 75°. The fabricated supporting dies are shown in Figs. 2 a, 2 b and 2 c respectively.

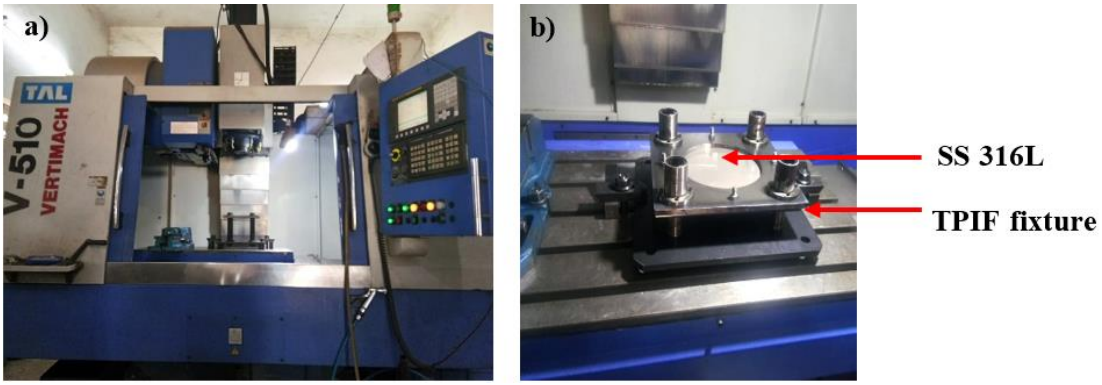

Figure 1: a) Vertimach V-510, b) TPIF setup.

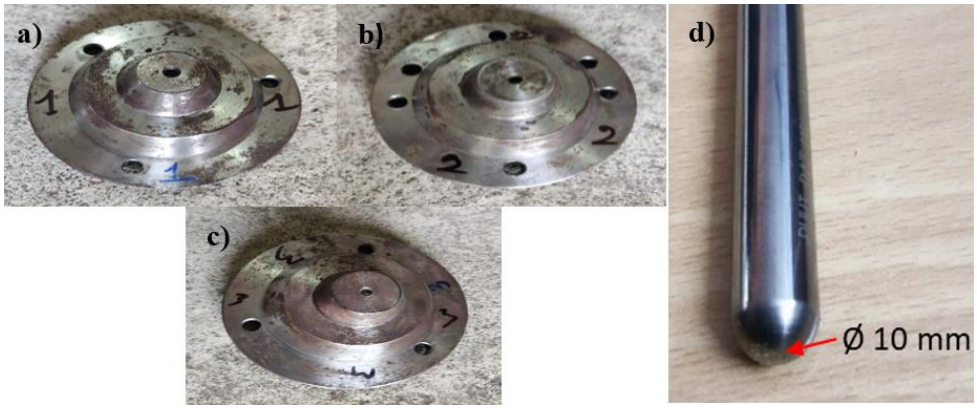

Figure 2: a), b) and c) TPIF forming dies with 70°, 73° and 75° top wall angles, d) forming tool.

SS316L Stainless steel sheets of size 280 mm × 280 mm with a thickness of 0.8 mm were used for the incremental forming process. A Tungsten Carbide tool of 10 mm nose diameter and 100 mm length as shown in Fig. 2 d was selected for the incremental forming process. The levels and the parameters chosen for the forming operation are shown in Table I. The TPIF experiments were performed for 9 different conditions as shown in Table II and the formed sheets are shown in Fig. 3.

Table I: Input parameters and their levels.

Parameter	Symbol	Unit	Code	Level 1 (L1)	Level 2 (L2)	Level 3 (L3)
Die angle	*DA*	(°)	A	70	73	75
Step of forming	*SD*	(mm)	B	0.2	0.3	0.4
Rate of feed	*FR*	(mm/min)	C	500	1000	1500
Tool rotational speed	*SS*	(rpm)	D	100	200	300

Table II: Experimental combinations and the obtained results.

Exp. No.	*DA* (°)	*SD* (mm)	*FR* (mm/min)	*SS* (rpm)	Ra_{top} (µm)	Ra_{middle} (µm)	Ra_{bottom} (µm)	Th_{top} (mm)	Th_{middle} (mm)	Th_{bottom} (mm)
1	70	0.2	500	100	0.422	0.421	0.436	0.751	0.689	0.462
2	70	0.3	1000	200	0.582	0.518	0.596	0.701	0.639	0.425
3	70	0.4	1500	300	0.807	0.836	0.898	0.712	0.665	0.432
4	73	0.2	500	200	0.542	0.568	0.525	0.725	0.652	0.436
5	73	0.3	1000	300	0.735	0.712	0.705	0.738	0.643	0.445
6	73	0.4	1500	100	0.625	0.642	0.655	0.749	0.648	0.447
7	75	0.2	1000	100	0.468	0.472	0.495	0.736	0.678	0.468
8	75	0.3	1500	200	0.428	0.445	0.438	0.725	0.668	0.452
9	75	0.4	500	300	0.669	0.658	0.662	0.741	0.687	0.458

Figure 3: TPIF formed components.

4. RESULTS AND DISCUSSION

4.1 The influence of process parameters on the average output responses

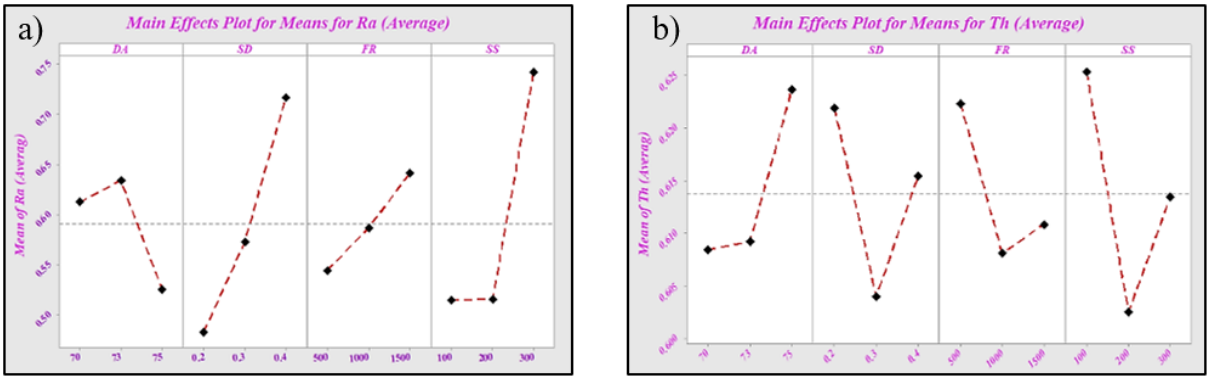

Figure 4: a) Mean of Ra_{avg} of varying process parameters, b) Mean of Th_{avg} of varying process parameters.

Fig. 4 a shows that the average surface roughness Ra_{avg} increases with the increase in the Die angle from 70° to 73° and then as the Die angle increases further to 75° the surface roughness Ra_{avg} tends to decrease. The graph also reveals that Ra_{avg} increases as the Step of forming increases from 0.2 mm to 0.4 mm. With an increase in the Rate of feed from 500 mm/min to 1500 mm/min the Ra_{avg} increases. Additionally, with an increase in Tool rotational speed of 100 rpm to 200 rpm, the Ra_{avg} shows no change whereas when the Tool rotational speed is increased from 200 rpm and 300 rpm the Ra_{avg} increases.

Fig. 4 b shows that the average thickness Th_{avg} increases with the increase in the Die angle from 70° to 75°. The graph also reveals that Th_{avg} decreases as the Step of forming increases from 0.2 mm to 0.3 mm and Th_{avg} increases as the Step of forming increases from 0.3 mm to 0.4 mm. With an increase in the Rate of feed from 500 mm/min to 1000 mm/min the Th_{avg}

decreases. When the Rate of feed is increased further from 1000 mm/min to 1500 mm/min the Th_{avg} increases. Th_{avg} decreases as the Tool rotational speed increase from 100 rpm to 200 rpm and subsequently, Th_{avg} is found to be increasing as the Tool rotational speed is further increased to 300 rpm.

4.2 Taguchi method

The Taguchi technique is an effective way to optimise the input parameters that reduces the number of experiments using orthogonal arrays. This study uses an L_9 orthogonal array since three input parameters at three levels were chosen. This tool evaluates data using the S/N ratio. The surface roughness was considered for smaller the better criterion which is calculated by Eq. (1). Similarly, the thickness is considered to be larger the better which is calculated by Eq. (2). The calculated Signal to Noise (S/N) ratio (η) for the two responses is shown in Table III. The symbol n represents the number of replicates and Y_{ij} represents the numerical value of the considered experimental run.

$$\text{S/N ratio } (\eta) = -10\log_{10}\left(\frac{1}{n}\right)\sum_{i=1}^{n}(Y_{ij}^2) \tag{1}$$

$$\text{S/N ratio } (\eta) = -10\log_{10}\left(\frac{1}{n}\right)\sum_{i=1}^{n}(1/Y_{ij}^2) \tag{2}$$

Table III: S/N ratio of the output responses.

Exp. No.	Ra_{top} (μm)	Ra_{middle} (μm)	Ra_{bottom} (μm)	Th_{top} (mm)	Th_{middle} (mm)	Th_{bottom} (mm)
1	7.4938	7.5144	7.2103	-2.4872	-3.2356	-6.7072
2	4.7015	5.7134	4.4951	-3.0856	-3.8900	-7.4322
3	1.8625	1.5559	0.9345	-2.9504	-3.5436	-7.2903
4	5.3200	4.9130	5.5968	-2.7932	-3.7150	-7.2103
5	2.6743	2.9504	3.0362	-2.6389	-3.8358	-7.0328
6	4.0824	3.8493	3.6752	-2.5104	-3.7685	-6.9938
7	6.5951	6.5212	6.1079	-2.6624	-3.3754	-6.5951
8	7.3711	7.0328	7.1705	-2.7932	-3.5045	-6.8972
9	3.4915	3.6355	3.5828	-2.6036	-3.2609	-6.7827

4.3 Grey Relational Analysis (GRA)

Multiple performance parameters were explored using a grey relational method in the present study. The following stages are done for this approach:

Step 1: The Normalization of the S/N ratios obtained from the Taguchi method can be carried out using Eqs. (3) and (4) for smaller the better and larger the better respectively as shown in Table IV.

$$\text{Normalised S/N ratio, } Z_{ij} = \frac{(MaxY_{ij} - Y_{ij})}{(MaxY_{ij} - MinY_{ij})} \tag{3}$$

$$\text{Normalised S/N ratio, } Z_{ij} = \frac{(Y_{ij} - MinY_{ij})}{(MaxY_{ij} - MinY_{ij})} \tag{4}$$

where, Y_{ij} is the numerical value of the considered experimental run and $MaxY_{ij}$ and $MinY_{ij}$ are the maximum and minimum among the values of the S/N ratio of the output responses.

Step 2: The Grey Relational Coefficient (*GRC*) can be calculated using Eq. (5) and shown in Table V.

$$\xi_{ij} = \frac{\Delta_{\min} + \lambda\Delta_{\max}}{\Delta_{ij} + \lambda\Delta_{\max}} \tag{5}$$

where, ξ_{ij} is the *GRC* and λ is the distinguishing coefficient, $(0 \leq \lambda \leq 1)$. Δ_{ij} is the corresponding value obtained from the deviational sequence for the selected trial.

Step 3: Grey Relational Grade (*GRG*) is calculated using Eq. (6) and shown in Table V.

$$G_i = \frac{1}{m}\sum_{j=1}^{m} \xi_{ij} \tag{6}$$

where, m is the number of responses considered, and ξ_{ij} represents the *GRC* values of all the responses of the individual experimental run.

Table IV: Normalised S/N ratio.

Exp. No.	Ra_{top} (µm)	Ra_{middle} (µm)	Ra_{bottom} (µm)	Th_{top} (mm)	Th_{middle} (mm)	Th_{bottom} (mm)
1	0.0000	0.0000	0.0000	1.0000	1.0000	0.8661
2	0.4958	0.3023	0.4326	0.0000	0.0000	0.0000
3	1.0000	1.0000	1.0000	0.2260	0.5294	0.1695
4	0.3860	0.4366	0.2571	0.4886	0.2673	0.2651
5	0.8559	0.7660	0.6651	0.7466	0.0828	0.4771
6	0.6058	0.6151	0.5633	0.9613	0.1856	0.5237
7	0.1596	0.1667	0.1757	0.7072	0.7864	1.0000
8	0.0218	0.0808	0.0063	0.4886	0.5891	0.6391
9	0.7107	0.6510	0.5780	0.8054	0.9614	0.7759

From Table V it can be seen that experiment No. 3 has the highest *GRG* of 0.7139 among all the experiments and hence Rank 1. The higher *GRG* will have better multi-response characteristics. The average *GRG* value for every level of the input parameters is shown in Table V. The same is shown in Fig. 5.

Table V: *GRC*, *GRG* and Rank.

Exp. No.	*GRC*						*GRG*	Rank
	Ra_{top} (µm)	Ra_{middle} (µm)	Ra_{bottom} (µm)	Th_{top} (mm)	Th_{middle} (mm)	Th_{bottom} (mm)		
1	0.3333	0.3333	0.3333	1.0000	1.0000	0.7888	0.6315	3
2	0.4979	0.4174	0.4684	0.3333	0.3333	0.3333	0.3973	9
3	1.0000	1.0000	1.0000	0.3925	0.5151	0.3758	0.7139	1
4	0.4488	0.4702	0.4023	0.4944	0.4056	0.4049	0.4377	8
5	0.7762	0.6812	0.5989	0.6636	0.3528	0.4888	0.5936	4
6	0.5592	0.5650	0.5338	0.9282	0.3804	0.5121	0.5798	5
7	0.3730	0.3750	0.3775	0.6306	0.7006	1.0000	0.5761	6
8	0.3382	0.3523	0.3347	0.4944	0.5489	0.5808	0.4416	7
9	0.6335	0.5889	0.5423	0.7199	0.9284	0.6905	0.6839	3

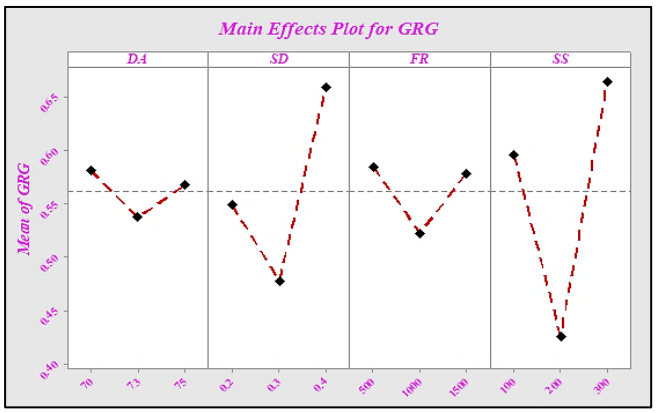

Figure 5: Main effects plot for *GRG* – GRA.

Table VI: Average *GRG* for responses.

Parameter	Symbol	Unit	Average *GRG*				Rank
			Level 1	Level 2	Level 3	Range	
Die angle	*DA*	(°)	**0.5809**	0.537	0.5672	0.0439	4
Step of forming	*SD*	(mm)	0.5484	0.4775	**0.6592**	0.1817	2
Rate of feed	*FR*	(mm/min)	**0.5844**	0.5223	0.5784	0.0621	3
Tool rotational speed	***SS***	(rpm)	0.5958	0.4255	**0.6638**	0.2383	**1**
Overall mean *GRG* = 0.5617							

The actual process parameter combination for getting better surface roughness and thickness is Die angle (*DA*-L1) at 70°, Step of forming (*SD*-L3) at 0.4 mm, Rate of feed (*FR*-L1) at 500 mm/min and Tool rotation speed (*SS*-L3) at 300 rpm as shown in Table VI. From Table VI, it can be seen that Tool rotational speed has the highest range among all the other parameters. Therefore, the Tool rotational speed has a higher influence on the output responses.

4.4 Confirmation experiments for GRA

The optimal predicted grey relational value is given by Eq. (7).

$$Y = Y_i + \sum (Y_n - Y_i) \tag{7}$$

where, Y_i is the mean *GRG*, Y_n is the mean *GRG* at optimal conditions.

Table VII: Values of the confirmational experiment.

Responses	Initial parameter combination	Optimal parameter combination	
		Prediction	Experimental
	(***DA***-L1) (***SD***-L1) (***FR***-L1) (***SS***-L1)	(***DA***-L1) (***SD***-L3) (***FR***-L1) (***SS***-L3)	(***DA***-L1) (***SD***-L3) (***FR***-L1) (***SS***-L3)
Ra_{top} (μm)	0.422	-	0.418
Ra_{middle} (μm)	0.421	-	0.412
Ra_{bottom} (μm)	0.436	-	0.415
Th_{top} (mm)	0.751	-	0.762
Th_{middle} (mm)	0.689	-	0.701
Th_{bottom} (mm)	0.458	-	0.512
Weighted *GRG*	0.6315	0.8032	0.9226
Improvement in *GRG* = 0.3145			

The above Table VII shows that the surface roughness has been reduced from 0.422 μm to 0.418 μm at Ra_{top} and from 0.421 μm to 0.412 μm at Ra_{middle} and from 0.436 μm to 0.415 μm at Ra_{bottom} regions. Also, the thickness has been increased from 0.751 mm to 0.762 mm at Th_{top} and from 0.689 mm to 0.701 mm at Th_{middle} and from 0.458 mm to 0.512 mm at Th_{bottom}. The results of the confirmation test are tabulated in Table VII and that obtained *GRG* was 0.9226. The predicted results have been calculated as 0.9575. The *GRG* value of the confirmation run was enhanced by 3.5 %. The proposed method has significantly reduced the surface roughness and increased the thickness of the formed components with an improvement in *GRG* of 0.3145.

4.5 Technique for Order of Preference by Similarity to Ideal Solution (TOPSIS)

Multiple Criteria Decision Making (MCDM) approaches have evolved as one of the most powerful and successful tools in the past decade for solving industrial issues with many criteria. They are used to determine the optimal solution among several choices. The optimal alternative

is most similar to the ideal solution and most dissimilar to the ideal solution. The TOPSIS method [18] can be constructed by following the steps given below:

Step 1: Determine the normalised matrix using Eq. (8).

$$N_{ij} = \frac{Y_{ij}}{\sqrt{\sum_{i=1}^{n} Y_{ij}^2}} \tag{8}$$

where, Y_{ij} is the actual value of the i^{th} experimental result for the j^{th} response and N_{ij} is the corresponding normalised value.

Step 2: Identify the weights and multiply with N_{ij} to obtain the weighted normalised matrix (B_{ij}) by applying Eq. (9).

$$B_{ij} = w_j \times N_{ij} \tag{9}$$

where, N_{ij} can be obtained from Eq. (8) and weights per attribute (w_j) are considered as 0.5 for all the experiments. Table VIII and Table IX shows the calculated values for the normalized and weighted matrix respectively.

Table VIII: Normalised matrix.

Exp. No.	Ra_{top} (μm)	Ra_{middle} (μm)	Ra_{bottom} (μm)	Th_{top} (mm)	Th_{middle} (mm)	Th_{bottom} (mm)
1	0.2344	0.2339	0.1901	0.2355	0.5640	0.3424
2	0.3232	0.2878	0.3552	0.3219	0.4914	0.3196
3	0.4482	0.4644	0.8064	0.4850	0.5069	0.3246
4	0.3010	0.3156	0.2756	0.2835	0.5256	0.3306
5	0.4082	0.3956	0.4970	0.3807	0.5446	0.3365
6	0.3471	0.3567	0.4290	0.3537	0.5610	0.3415
7	0.2599	0.2622	0.2450	0.2673	0.5417	0.3356
8	0.2377	0.2472	0.1918	0.2365	0.5256	0.3306
9	0.3715	0.3656	0.4382	0.3575	0.5491	0.3379

Step 3: Calculation of the Positive ideal solution (P_j^+) and the Negative ideal solution (P_j^-) using Eqs. (10) and (11) respectively.

$$P_j^+ = [P_1^+, ..., P_n^+]$$

$$\text{where, } P_i^+ = [\{max\,(P_{ij}) \text{ if } j \in J\}, \{min\,(P_{ij}) \text{ if } j \in J^\$\}] \tag{10}$$

$$P_j^- = [P_1^-, ..., P_n^-]$$

$$\text{where, } P_i^- = [\{min\,(P_{ij}) \text{ if } j \in J\}, \{max\,(P_{ij}) \text{ if } j \in J^\$\}] \tag{11}$$

where, $J^\$$ implies cost criteria and J implies beneficial criteria.

Step 4: Separation value from Positive ideal solutions (V^+) and Separation value from Negative ideal solutions (V^-) are calculated using Eqs. (12) and (13) and shown in Table IX.

$$V^+ = \sqrt{\sum_{j=1}^{n} (B_{ij} - P_i^+)^2} \tag{12}$$

$$V^- = \sqrt{\sum_{j=1}^{n} (B_{ij} - P_i^-)^2} \tag{13}$$

Step 5: Determination of the Relative Closeness coefficient (*RCC*) using Eq. (14). It is shown in Table IX.

$$RCC_i = \frac{V_i^-}{(V_i^+ + V_i^-)} \tag{14}$$

The larger the Relative Closeness C_i value shows closer to the optimum performance of the alternatives.

Step 6: The highest value of the Closeness coefficient is experienced in Experiment 1, therefore, it is ranked 1 as shown in Table IX.

Table IX: Weighted normalised matrix, Ideal solution, Closeness coefficient with Rank.

Exp. No.	Weighted normalised matrix						V^+	V^-	RCC_i	Rank
	Ra_{top} (µm)	Ra_{middle} (µm)	Ra_{bottom} (µm)	Th_{top} (mm)	Th_{middle} (mm)	Th_{bottom} (mm)				
1	0.1172	0.1169	0.1177	0.1712	0.1731	0.1721	0.5976	0.2019	0.3302	**1**
2	0.1616	0.1439	0.1609	0.1598	0.1605	0.1583	0.5797	0.1355	0.2337	5
3	0.2241	0.2322	0.2425	0.1623	0.1671	0.1609	0.6161	0.0075	0.0121	9
4	0.1505	0.1578	0.1418	0.1653	0.1638	0.1624	0.5861	0.1455	0.2465	4
5	0.2041	0.1978	0.1904	0.1682	0.1615	0.1658	0.6019	0.0666	0.1092	8
6	0.1735	0.1783	0.1769	0.1708	0.1628	0.1665	0.5970	0.0998	0.1649	6
7	0.1300	0.1311	0.1337	0.1678	0.1703	0.1743	0.5958	0.1770	0.2893	3
8	0.1188	0.1236	0.1183	0.1653	0.1678	0.1684	0.5890	0.1962	0.3275	2
9	0.1858	0.1828	0.1788	0.1689	0.1726	0.1706	0.6057	0.0914	0.1479	7

Table X: Response table for Closeness coefficient with appropriate Rank.

Parameter	Symbol	Unit	Average *GRG*				Rank
			Level 1	Level 2	Level 3	Range	
Die angle	*DA*	(°)	0.192	0.1735	**0.2549**	0.0814	3
Step of forming	***SD***	(mm)	**0.2887**	0.2235	0.1083	0.1804	**1**
Rate of feed	*FR*	(mm/min)	**0.2415**	0.2108	0.1681	0.0734	4
Tool rotational speed	*SS*	(rpm)	0.2615	**0.2692**	0.0897	0.1795	2

The most influencing process parameter will be selected based on the variation having the highest value of the mean of Closeness coefficient. From Table X the actual process parameter combination for getting better surface roughness and higher thickness is Die angle (*DA*-L3) at 73°, Step of forming (*SD*-L1) at 0.2 mm, Rate of feed (*FR*-L1) at 500 mm/min and Tool rotation speed (*SS*-L2) at 200 rpm. From Table X it can be seen that the Step of forming (*SD*) has the highest range among all the other parameters. Therefore, the Tool rotational speed has a higher influence on the output responses. The same is shown in Fig. 6.

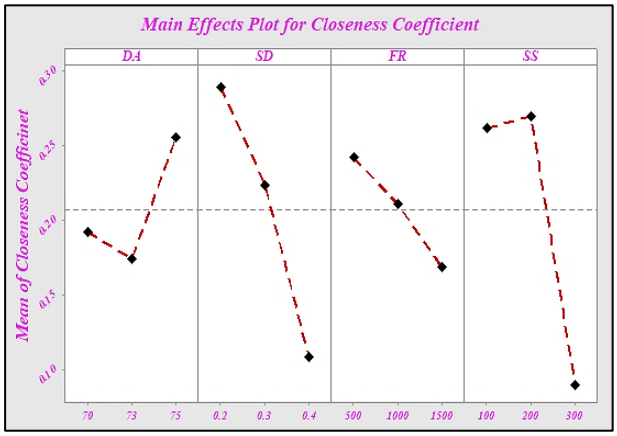

Figure 6: Main effect plot for Closeness coefficient.

4.6 Confirmation experiment for TOPSIS

The confirmation run for the identified process parameters using the TOPSIS approach was performed and the out responses were studied and the values are given in Table XI.

Table XI: Values of the Confirmational experiment.

Responses	Initial Parameter Combination	Optimal Parameter Combination
		Experimental
	(*DA*-L1) (*SD*-L1) (*FR*-L1) (*SS*-L1)	(*DA*-L3) (*SD*-L1) (*FR*-L1) (*SS*-L2)
Ra_{top} (μm)	0.422	0.418
Ra_{middle} (μm)	0.421	0.411
Ra_{bottom} (μm)	0.436	0.402
Th_{top} (mm)	0.751	0.769
Th_{middle} (mm)	0.689	0.754
Th_{bottom} (mm)	0.458	0.614
Weighted *GRG*	0.3302	0.4626
Improvement in *GRG* = 0.1324		

Table XI shows that the surface roughness has been reduced from 0.422 μm to 0.418 μm at Ra_{top} and from 0.421 μm to 0.411 μm at Ra_{middle} and from 0.436 μm to 0.402 μm at Ra_{bottom} regions. Also, the thickness has been increased from 0.751 mm to 0.769 mm at Th_{top} and from 0.689 mm to 0.754 mm Th_{middle} and from 0.458 mm to 0.614 mm at Th_{bottom}. The proposed method has improved both surface roughness and thickness of the formed components with an improvement in *GRG* of 0.1324.

4.7 ANOVA for GRA and TOPSIS

ANOVA is incorporated to determine the maximum contributing factor for the responses considered. Table XII shows the ANOVA for *GRG* calculated using GRA and Closeness coefficient using TOPSIS. It can be seen that Tool rotational speed (*SS*) has the highest contribution of 30.55 % followed by Rate of feed (*FR*), Depth of forming (*SD*) and Die angle (*DA*) having 28.65 %, 23.65 % and 15.14 % respectively. Additionally, Table XII shows the ANOVA for the Closeness coefficient calculated using TOPSIS. It can be seen that the Step of forming (*SD*) has the highest percentage contribution of 31.3 % followed by the Rate of feed, Tool rotational speed (*FR*) and Die angle (*DA*) each having 26.3 %, 21.3 % and 20.3 % respectively. Therefore, Tool rotation speed (*SS*) and Step of forming (*SD*) are having the highest influence on the output responses based on *GRG* and TOPSIS respectively.

Table XII: ANOVA for *GRG* and Closeness coefficient.

GRG					**Closeness coefficient**				
Source	***DF***	**Sum of square**	**Mean square**	**Contribution**	**Source**	***DF***	**Sum of square**	**Mean square**	**Contribution**
DA	2	0.000513	0.000513	15.14 %	*DA*	2	0.004683	0.004683	20.3 %
SD	2	0.018401	0.019071	23.65 %	***SD***	2	0.048798	0.010028	**31.3 %**
FR	2	0.007521	0.007340	28.65 %	*FR*	2	0.000566	0.000242	26.3 %
SS	2	0.000138	0.000138	**30.55 %**	*SS*	2	0.012977	0.012977	21.3 %
Error	2	0.074781	0.018695	2.01 %	Error	2	0.024537	0.006134	1.2 %
Total	10	0.101843	-	-	Total	10	0.091561	-	-

5. CONCLUSION AND FUTURE WORK

The present work was carried out to investigate the influence of process parameter on surface roughness and thickness of the TPIF-formed components. The performed experiments were constructed using the Taguchi DOE technique and the multi-response optimization was

performed using Grey Relational Analysis and TOPSIS method. The following points are inferred from the above investigations:

a) The predicted optimum process parameters through the GRA method were found to be at a Die angle of 70° (*DA*-L1), Step of forming of 0.4 mm (*SD*-L3), Rate of feed of 500 mm/min (*FR*-L1) and Tool rotational speed (*SS*-L3) of 300 rpm, whereas through TOPIS the optimum process parameters were found to be Die angle of 73° (*DA*-L3), Step of forming of 0.2 mm (*SD*-L1), Rate of feed of 500 mm/min (*FR*-L1) and Tool rotational speed (*SS*-L2) of 200 rpm.
b) At a confidence level of 95 %, by implementing the ANOVA method, the Tool rotational speed and Step of forming were found to most significant factors for GRA and TOPSIS methods respectively.
c) The improvement in *GRG* was 0.3145 using GRA and the improvement in Closeness coefficient was 0.1324. Both the methods have improvements in the multi-response characteristics.

The optimum process parameters proposed by GRA and TOPSIS methods has significant improvement in the output responses of the TPIF-formed components. Therefore, both the methods are further encouraged for achieving better results for the given combination of input parameters. In future this research can be extended by varying the diameter of the forming tool, varying the thickness of the workpiece, changing the lubricant, etc. Responses such as wall angle of the formed workpiece, forming height and strain developed can be briefly investigated.

REFERENCES

[1] Ficko, M.; Begic Hajdarevic, D.; Hadziabdic, V.; Klancnik, S. (2020). Multi-response optimisation of turning process parameters with GRA and TOPSIS methods, *International Journal of Simulation Modelling*, Vol. 19, No. 4, 547-558, doi:10.2507/IJSIMM19-4-524

[2] Al-Shayea, A.; Dabwan, A.; Ragab, A. E.; Nasr, M. M.; Kaid, H. (2019). Studying the effect of process parameters on part depth in single point incremental forming of AA1050-H14 aluminum alloy sheets, *Technical Gazette*, Vol. 26, No. 6, 1606-1613, doi:10.17559/TV-20180114203921

[3] Nasulea, D.; Oancea, G. (2018). Integrating a new software tool used for tool path generation in the numerical simulation of incremental forming processes, *Strojniski vestnik – Journal of Mechanical Engineering*, Vol. 64, No. 10, 643-651, doi:10.5545/sv-jme.2018.5475

[4] Pratheesh Kumar, S.; Elangovan, S. (2020). Optimization in single point incremental forming of Inconel 718 through response surface methodology, *Transactions of the Canadian Society for Mechanical Engineering*, Vol. 44, No. 1, 148-160, doi:10.1139/tcsme-2019-0003

[5] Ou, L.; An, Z.; Gao, Z.; Zhou, S.; Men, Z. (2020). Effects of process parameters on the thickness uniformity in Two-Point Incremental Forming (TPIF) with a positive die for an irregular stepped part, *Materials*, Vol. 13, No. 11, 19 pages, doi:10.3390/ma13112634

[6] Maji, K.; Kumar, G. (2020). Inverse analysis and multi-objective optimization of single-point incremental forming of AA5083 aluminum alloy sheet, *Soft Computing*, Vol. 24, No. 6, 4505-4521, doi:10.1007/s00500-019-04211-z

[7] Esmailian, M.; Khalili, K. (2020). Prediction of tool force in two point incremental forming by slab analysis, *International Journal of Engineering*, Vol. 33, No. 11, 2399-2407, doi:10.5829/ije.2020.33.11b.30

[8] Choi, H.; Lee, C. (2019). A mathematical model to predict thickness distribution and formability of incremental forming combined with stretch forming, *Robotics and Computer-Integrated Manufacturing*, Vol. 55, Part B, 164-172, doi:10.1016/j.rcim.2018.07.014

[9] Kumar, A.; Gulati, V. (2019). Experimental investigation and optimization of surface roughness in negative incremental forming, *Measurement*, Vol. 131, 419-430, doi:10.1016/j.measurement.2018.08.078

[10] Dakhli, M.; Boulila, A.; Manach, P.-Y.; Tourki, Z. (2019). Optimization of processing parameters and surface roughness of metallic sheets plastically deformed by incremental forming process, *The*

International Journal of Advanced Manufacturing Technology, Vol. 102, No. 1-4, 977-990, doi:10.1007/s00170-018-03265-x

[11] Kumar, A.; Gulati, V. (2018). Experimental investigations and optimization of forming force in incremental sheet forming, *Sadhana*, Vol. 43, No. 10, Paper 159, 15 pages, doi:10.1007/s12046-018-0926-7

[12] Mostafanezhad, H.; Menghari, H. G.; Esmaeili, S.; Shirkharkolaee, E. M. (2018). Optimization of two-point incremental forming process of AA1050 through response surface methodology, *Measurement*, Vol. 127, 21-28, doi:10.1016/j.measurement.2018.04.042

[13] Li, Z.; Lu, S.; Zhang, T.; Mao, Z.; Zhang, C. (2018). A simple and low-cost lubrication method for improvement in the surface quality of incremental sheet metal forming, *Transactions of the Indian Institute of Metals*, Vol. 71, No. 7, 1715-1719, doi:10.1007/s12666-018-1305-0

[14] Torres, S.; Ortega, R.; Acosta, P.; Calderón, E. (2021). Hot incremental forming of biocomposites developed from linen fibres and a thermoplastic matrix, *Strojniski vestnik – Journal of Mechanical Engineering*, Vol. 67, No. 3, 123-132, doi:10.5545/sv-jme.2020.6936

[15] Li, L.; Wang, J.; Wang, B. (2017). Geometric accuracy of incremental sheet forming for TRIP590, *Journal of Mechanical Science and Technology*, Vol. 31, No. 11, 5257-5264, doi:10.1007/s12206-017-1018-z

[16] Baruah, A.; Pandivelan, C.; Jeevanantham, A. K. (2017). Optimization of AA5052 in incremental sheet forming using grey relational analysis, *Measurement*, Vol. 106, 95-100, doi:10.1016/j.measurement.2017.04.029

[17] Mulay, A.; Satish Ben, B.; Ismail, S.; Kocanda, A. (2017). Experimental investigation and modeling of single point incremental forming for AA5052-H32 aluminum alloy, *Arabian Journal of Science and Engineering*, Vol. 42, No. 11, 4929-4940, doi:10.1007/s13369-017-2746-1

[18] Nagarajan, V.; Solaiyappan, A.; Mahalingam, S. K.; Nagarajan, L.; Salunkhe, S.; Nasr, E. A.; Shanmugam, R.; Moneam Hussein, H. H. A. (2022). Meta-heuristic technique-based parametric optimization for electrochemical machining of Monel 400 alloys to investigate the material removal rate and the sludge, *Applied Sciences*, Vol. 12, No. 6, Paper 2793, 23 pages, doi:10.3390/app12062793